



# Kent Academic Repository

Lai, Huadong, Liu, Mingxing, Xu, Jinqiang, Luo, Peng, Chen, Changrun and Xu, Weichao (2024) *Improved Weighted Covariance Based Detector for Spectrum Sensing in Rayleigh Fading Channel*. *IEEE Wireless Communications Letters*. ISSN 2162-2337.

## Downloaded from

<https://kar.kent.ac.uk/105482/> The University of Kent's Academic Repository KAR

## The version of record is available from

<https://doi.org/10.1109/lwc.2024.3379528>

## This document version

Author's Accepted Manuscript

## DOI for this version

## Licence for this version

UNSPECIFIED

## Additional information

© 2024 IEEE. Personal use of this material is permitted. Permission from IEEE must be obtained for all other uses, in any current or future media, including reprinting/republishing this material for advertising or promotional purposes, creating new collective works, for resale or redistribution to servers or lists, or reuse of any copyrighted component of this work in other works.

## Versions of research works

### Versions of Record

If this version is the version of record, it is the same as the published version available on the publisher's web site. Cite as the published version.

### Author Accepted Manuscripts

If this document is identified as the Author Accepted Manuscript it is the version after peer review but before type setting, copy editing or publisher branding. Cite as Surname, Initial. (Year) 'Title of article'. To be published in **Title of Journal**, Volume and issue numbers [peer-reviewed accepted version]. Available at: DOI or URL (Accessed: date).

## Enquiries

If you have questions about this document contact [ResearchSupport@kent.ac.uk](mailto:ResearchSupport@kent.ac.uk). Please include the URL of the record in KAR. If you believe that your, or a third party's rights have been compromised through this document please see our [Take Down policy](https://www.kent.ac.uk/guides/kar-the-kent-academic-repository#policies) (available from <https://www.kent.ac.uk/guides/kar-the-kent-academic-repository#policies>).

# Improved Weighted Covariance-Based Detector for Spectrum Sensing in Rayleigh Fading Channel

AQ1 Huadong Lai<sup>ID</sup>, Mingxing Liu<sup>ID</sup>, *Member, IEEE*, Jinqiang Xu, Peng Luo<sup>ID</sup>, Changrun Chen<sup>ID</sup>, and Weichao Xu<sup>ID</sup>

1 **Abstract**—In this letter, we propose an improved weighted  
 2 covariance based detector (IWCD) for spatially correlated time-  
 3 varying Rayleigh fading channel. The proposed method uses  
 4 adaptive weights that are tailored to the dynamic nature of  
 5 the channels. These weights can be chosen manually to meet  
 6 practical requirements or derived theoretically by optimizing  
 7 some performance index, such that the IWCD outperforms  
 8 traditional weighted covariance-based detectors (WCDs), which  
 9 rely heavily on data-aided weights determined by the sample  
 10 covariance matrix (SCM). Performance merits in terms of the  
 11 probabilities of false alarm and detection are analyzed in the  
 12 low signal-to-noise-ratio (SNR) regime. Besides, the optimal  
 13 weights are derived via maximizing the modified deflection  
 14 coefficient (MDC). A reasonable estimator of the optimal weights  
 15 is also constructed armed with the available samples at hand.  
 16 Theoretical analyses and experimental results demonstrate the  
 17 superiority of our proposed method over existing works in  
 18 various scenarios.

19 **Index Terms**—Spectrum sensing, weighted covariance based  
 20 detector, rayleigh fading channel, modified deflection coefficient.

## 21 I. INTRODUCTION

22 **C**OGNITIVE radio (CR), which allows the unlicensed sec-  
 23 ondary users to utilize the idle spectrum bands originally  
 24 allocated to but not occupied by the licensed primary users,  
 25 is recognized as a promising network architecture to improve  
 26 the spectrum utilization efficiency and alleviate the problem  
 27 of spectrum scarcity [1], [2], [3]. Spectrum sensing, as one of  
 28 the most important functionalities of CR, aims at seeking the  
 29 idle frequency band via continuously monitoring the activity  
 30 state of PUs [4].

31 Traditional energy detection is widely utilized for spec-  
 32 trum sensing owing to its low computational complexity  
 33 and simplicity of implementation. However, the performance

of ED will degrade considerably in the presence of noise 34  
 uncertainty [5]. To overcome it, a variety of robust spectrum 35  
 sensing schemes have been addressed in the literature, such 36  
 as the correlation-based detector (covariance absolute value 37  
 (CAV) [6], volume based detection (VOL) [7], hadamard ratio 38  
 test (HDM) [8]) and the machine learning-based schemes 39  
 (CNN-LSTM [9] and CM-CNN [10]). By assuming the 40  
 quasi-static fading channels, these approaches are capable 41  
 of delivering desirable performance gain, but they may suffer 42  
 from performance deterioration when the transmission 43  
 channel is time-varying fading. To this end, several research 44  
 efforts in the aspect of weighted covariance are addressed 45  
 for time-varying fading channel, such as complex-valued 46  
 WCD (CWCD) [11], real-valued WCD (RWCD) [12], gen- 47  
 eralization RWCD (GRWCD) [13] and modified GRWCD 48  
 (MGRWCD) [13]. The pivotal idea is to construct the WCD- 49  
 based statistic by employing the SCM-based weights within 50  
 the principle of CAV. The performance of WCDs can be 51  
 significantly enhanced by employing the SCM-aided weights 52  
 to reduce the overlap between the distributions of test statistic 53  
 with and without primary signals. However, the weights arising 54  
 from the SCM are deterministic and fixed, and a heuristic 55  
 method for achieving remarkable performance gain is to find 56  
 the more flexible combined weights that are tailored to the 57  
 time-varying channel. 58

Inspired by it, in this letter, an improved weighted covari- 59  
 ance based detector (IWCD) is addressed for the time-varying 60  
 correlated channels. Compared to the traditional data-aided 61  
 WCDs, the proposed method exhibits the wider degree of 62  
 flexibility because the utilized weights can be determined 63  
 by manual selection for practical demands or by theoretical 64  
 deduction via the optimization of some performance index. 65  
 The analytic expressions of the false alarm probability and 66  
 detection probability are derived in the scenarios where the 67  
 SNR is low. Then, an optimization problem based on MDC 68  
 is formulated, armed with which the optimal weights can 69  
 be determined. In addition, the optimal weights are reason- 70  
 ably estimated after estimating the unknown parameters from 71  
 the available samples. Numerical examples reveal that the 72  
 proposed IWCD method is superior to other state-of-the-art 73  
 detectors available in the literature. 74

*Notation:* The operators  $\text{tr}(\cdot)$ ,  $|\cdot|$ ,  $(\cdot)^*$ ,  $(\cdot)^T$  and  $(\cdot)^H$  denote 75  
 trace, modulus, conjugate, transpose and conjugate transpose, 76  
 respectively. The symbols of  $\mathbb{E}(x)$  and  $\mathbb{V}(x)$  are utilized to 77  
 represent the mean and variance of a random variable  $x$ .  $\mathbf{x} \sim$  78  
 $\mathcal{N}(\mu, \Sigma)$  ( $\mathcal{CN}(\mu, \Sigma)$ ) means that  $\mathbf{x}$  follows the real (complex) 79  
 Gaussian distribution with mean  $\mu$  and covariance matrix  $\Sigma$ , 80  
 whereas  $\sim$  signifies “distributed as”. The real and imaginary 81

AQ2 Manuscript received 9 January 2024; accepted 15 March 2024. This work  
 was supported in part by the Program for Scientific Research Start-Up Funds  
 of Guangdong Ocean University under Grant 060302112316, and in part by  
 the National Natural Science Foundation of China under Grant 62171143  
 and Grant 62171141. The associate editor coordinating the review of this  
 article and approving it for publication was J. Lee. (*Corresponding authors:*  
*Changrun Chen; Mingxing Liu.*)

Huadong Lai, Mingxing Liu, Jinqiang Xu, and Peng Luo are with  
 the School of Electronics and Information Engineering, Guangdong  
 Ocean University, Zhanjiang 524088, Guangdong, China (e-mail: hdlai@  
 gdou.edu.cn; liumx@gdou.edu.cn; xujinqiang1@163.com; luopeng@  
 gdou.edu.cn).

Changrun Chen is with the School of Engineering, University of Kent, CT2  
 7NT Canterbury, U.K. (e-mail: c.chen@kent.ac.uk).

Weichao Xu is with the Department of Automatic Control, School of  
 Automation, Guangdong University of Technology, Guangzhou 510006,  
 Guangdong, China (e-mail: wxu@gdut.edu.cn).

Digital Object Identifier 10.1109/LWC.2024.3379528

parts of  $x$  are denoted by  $\text{Re}(x)$  and  $\text{Im}(x)$ , respectively. We utilize  $\mathbf{0}_M$  and  $\mathbf{I}_M$  to represent the  $M \times 1$  zero vector and  $M \times M$  identity matrix.  $\Psi(x)$  and  $\Gamma(\cdot)$  correspond to a special confluent hypergeometric function  ${}_1F_1(-1/2, 1, x)$  and Gamma function [14], respectively. The  $\text{diag}\{\mathbf{x}\}$  stands for a diagonal matrix with diagonal elements consisting of  $x$ .

## II. PRELIMINARIES

### A. Problem Formulation

Herein we consider the detection of primary signal for a CR system that composes of one PU and one SU equipped with  $M$  sensing antennas through time-varying Rayleigh fading channel. Denote the absence and presence of primary signal in a specific frequency band by  $\mathcal{H}_0$  and  $\mathcal{H}_1$ , respectively. Under the above binary hypothesis, the observation vector  $\mathbf{x}(k)$  from  $M$ -antenna SU at time instant  $k$  can be expressed as [15]

$$\begin{cases} \mathcal{H}_0 : \mathbf{x}(k) = \mathbf{w}(k) \\ \mathcal{H}_1 : \mathbf{x}(k) = \mathbf{h}(k)s(k) + \mathbf{w}(k), \end{cases} k = 1, 2, \dots, K, \quad (1)$$

where  $s(k) \sim \mathcal{CN}(0, \sigma_s^2(k))$ , denotes the transmitted PU signal which is deterministic but unknown with instantaneous power  $\sigma_s^2(k)$ ;  $\mathbf{h}(k) \sim \mathcal{CN}(\mathbf{0}_M, \sigma_h^2 \Phi)$  represents the correlated Rayleigh fading channel with  $\sigma_h^2$  and  $\Phi$  being the channel power and normalized correlation matrix, respectively;  $\mathbf{w}(k) \sim \mathcal{CN}(\mathbf{0}_M, \mathbf{R}_w)$  is the additive background noise with unknown diagonal covariance matrix  $\mathbf{R}_w = \text{diag}\{\sigma_1^2, \dots, \sigma_M^2\}$ . Generally, it is assumed that  $s(k)$ ,  $\mathbf{h}(k)$  and  $\mathbf{w}(k)$  are statistically independent with each other.

### B. Channel Model

Due to its simplicity and excellent characterization of spatial correlation, the antenna correlation matrix  $\Phi$  is typically described by exponential correlation model [15], i.e.,

$$\Phi_{mn} = \begin{cases} \rho^{n-m}, & m \leq n \\ \Phi_{nm}^*, & m > n \end{cases}, m, n = 1, 2, \dots, M, \quad (2)$$

where  $|\rho| \leq 1$  is the complex-valued correlation coefficient between two neighboring antennas.

In such occasion, the channel vector  $\mathbf{h}(k)$  is generated as

$$\mathbf{h}(k) = \Phi^{\frac{1}{2}} \mathbf{g}(k), k = 1, 2, \dots, N, \quad (3)$$

where  $\mathbf{g}(k) \sim \mathcal{CN}(\mathbf{0}_M, \mathbf{I}_M)$ , denotes the standard complex Gaussian distributed random vector.

## III. TEST STATISTIC AND PERFORMANCE ANALYSIS

This section first briefly reviews weighted covariance-based sensing algorithms framework, and then elaborates the proposed test statistic. Besides, performance measures for the probabilities of false alarm probability and detection are studied in the low SNR regime with the assistance of central limit theorem (CLT) [16]. Finally, the optimal weights are computed via the optimization problem based on MDC [17], an estimate of which is also obtained with the available samples.

### A. Improved Weighted Covariance Based Detection

It is stated in [11], [12], [13] that the test statistics of WCDs are constructed by means of applying different weights to the entries of normalized SCM, i.e.,  $T_{\text{WCD}} \triangleq \sum_{i=1}^{M-1} \omega_i \sum_{n-m=i} |r'_{mn}|$  where  $r'_{mn} = r_{mn}/\hat{\sigma}^2$  with  $\hat{\sigma}^2 = \sum_{m=1}^M r_{mm}/M$  and  $r_{mn}$  being the  $(m, n)$  entries of SCM defined as  $\mathbf{R} = \frac{1}{K} \sum_{i=1}^K \mathbf{x}(k)\mathbf{x}^H(k)$ , and  $\omega_i$  is the weight obtained from the SCM. The data-aided weights can reduce the overlap between the distributions of detection statistic with and without the primary signal, thereby improving the detection power. However, the weights from the SCM are deemed to be fixed and unalterable, and a natural idea to achieve the better performance is to adopt the more flexible strategy with alterable weights, leading to our proposed method, as

$$T_{\text{IWCD}} \triangleq \sum_{i=0}^{M-1} \omega_i \sum_{n-m=i} |r_{mn}| \frac{\mathcal{H}_1}{\mathcal{H}_0} \lambda, \quad (4)$$

where  $\lambda$  is the decision threshold for a given false alarm probability,  $\{\omega_i\}_{i=0}^{M-1}$  are the weights, which play a pivotal role in improving the performance of our detection scheme. The weights can be manually prescribed according to practical requirements or theoretically determined by optimizing some performance index. Note that when  $\omega_0 = 0$ , IWCD reduces to CAV for  $\omega_i = 1/M$  ( $i = 1, \dots, M-1$ ), or reduces to CWCD for  $\omega_i = 4 \sum_{n-m=i} \text{Re}(r_{mn})/\hat{\sigma}^4$  ( $i = 1, \dots, M-1$ ).

### B. False Alarm Probability

We first establish the closed-form expression for the false alarm probability by following along the line in [18]. Specifically, in the scenario of low SNR and large  $K$ ,  $\{r_{mm}\}_{m=1}^M$  and  $\{r_{mn}\}_{n-m=1}^{M-1}$  are statistically independent, with PDFs:

$$r_{mm} | \mathcal{H}_0 \sim \mathcal{N}\left(\sigma_m^2, \frac{1}{K} \sigma_m^4\right), \quad (5)$$

$$r_{mn} | \mathcal{H}_0 \sim \mathcal{CN}\left(0, \frac{1}{K} \sigma_m^2 \sigma_n^2\right), \quad (6)$$

where  $\sigma_m^2$  and  $\sigma_n^2$  are  $m$ -th and  $n$ -th diagonal elements in  $\mathbf{R}_w$ .

Denote  $T_i \triangleq \sum_{n-m=i} |r_{mn}|$ , it is very easy to obtain

$$\mathbb{E}(T_0 | \mathcal{H}_0) = \sum_{m=1}^M \mathbb{E}[|r_{mm}|] = \sum_{m=1}^M \sigma_m^2, \quad (7)$$

$$\mathbb{V}(T_0 | \mathcal{H}_0) = \sum_{m=1}^M \mathbb{V}[|r_{mm}|] = \frac{1}{K} \sum_{m=1}^M \sigma_m^4. \quad (8)$$

The amplitude  $|r_{mn}|$  for  $n > m$ , follows the Rayleigh distribution with scale parameter  $\tilde{\sigma} = \frac{\sigma_m \sigma_n}{\sqrt{2K}}$ , whose first few raw moments are  $\mathbb{E}(|r_{mn}|^j) = \tilde{\sigma}^j 2^{\frac{j}{2}} \Gamma(1 + \frac{j}{2})$  [19].

We then obtain  $T_i$  for  $i = 1, \dots, M-1$ ,

$$\mathbb{E}[T_i | \mathcal{H}_0] = \sum_{n-m=i} \mathbb{E}[|r_{mn}|] = \sqrt{\frac{\pi}{4K}} \sum_{m=1}^{M-i} \sigma_m \sigma_{m+i}, \quad (9)$$

$$\mathbb{V}[T_i | \mathcal{H}_0] = \sum_{n-m=i} \mathbb{V}[|r_{mn}|] = \frac{4-\pi}{4K} \sum_{m=1}^{M-i} \sigma_m^2 \sigma_{m+i}^2. \quad (10)$$

169 The mean (denoted by  $\mu_0$ ) and variance (denoted by  $\sigma_0^2$ ) of  
170  $T_{\text{IWCD}}$  under  $\mathcal{H}_0$  can be respectively computed as

$$\begin{aligned} 171 \mu_0 &= \sum_{i=0}^{M-1} \mathbb{E}[\omega_i T_i | \mathcal{H}_0] \\ 172 &= \omega_0 \sum_{m=1}^M \sigma_m^2 + \sqrt{\frac{\pi}{4K}} \sum_{i=1}^{M-1} \omega_i \sum_{m=1}^{M-i} \sigma_m \sigma_{m+i}, \quad (11) \end{aligned}$$

$$\begin{aligned} 173 \sigma_0^2 &= \sum_{i=0}^{M-1} \mathbb{V}[\omega_i T_i | \mathcal{H}_0] \\ 174 &= \frac{\omega_0^2}{K} \sum_{m=1}^M \sigma_m^4 + \frac{4-\pi}{4K} \sum_{i=1}^{M-1} \omega_i^2 \sum_{m=1}^{M-i} \sigma_m^2 \sigma_{m+i}^2. \quad (12) \end{aligned}$$

175 Based on CLT, The distribution of IWCD can be computed as

$$176 T_{\text{IWCD}} | \mathcal{H}_0 \sim \mathcal{N}(\mu_0, \sigma_0^2). \quad (13)$$

177 When the threshold  $\lambda$  is pre-given, the false alarm  
178 probability is computed as

$$179 P_f = \Pr(T_{\text{IWCD}} > \lambda) = Q\left(\frac{\lambda - \mu_0}{\sigma_0}\right), \quad (14)$$

180 where  $Q(x) \triangleq \frac{1}{\sqrt{2\pi}} \int_x^{+\infty} e^{-\frac{u^2}{2}} du$  is the Gaussian-Q function.

181 Denote by  $Q^{-1}(\cdot)$  the inverse function of  $Q(\cdot)$ . The decision  
182 threshold can be evaluated with a prescribed  $P_f$ , as

$$183 \lambda = \sigma_0 Q^{-1}(P_f) + \mu_0. \quad (15)$$

### 184 C. Detection Probability

185 The analytic form for the probability of detection are  
186 investigated in this subsection. To continue, the lemma below  
187 is required to establish the distribution of  $r_{mn}$  under  $\mathcal{H}_1$ .

188 *Lemma 1:* Let  $\rho_i \triangleq \rho^{n-m}$  for  $n \geq m$ ,  $\sigma_{sh}^2(k) \triangleq \sigma_s^2(k)\sigma_h^2$ ,  
189  $\sigma_{sh}^2 \triangleq \frac{1}{K} \sum_{k=1}^K \sigma_{sh}^2(k)$ ,  $\tilde{\sigma}_m^2 \triangleq \sigma_{sh}^2 + \sigma_m^2$  and  $\tilde{\sigma}_n^2 \triangleq \sigma_{sh}^2 +$   
190  $\sigma_n^2$ . The SNR is defined as  $\text{SNR} = 10 \log_{10} \left( \frac{\sigma_{sh}^2}{\frac{1}{M} \text{tr}(\mathbf{R}_w)} \right)$ .

191 Then, when  $\mathcal{H}_1$  holds,  $\{r_{mm}\}_{m=1}^M$  and  $\{r_{mn}\}_{n=m+1}^{M-1}$  are  
192 mutually independent in the low SNR regime, whose PDFs  
193 are respectively given by

$$194 r_{mm} | \mathcal{H}_1 \sim \mathcal{N}\left[\tilde{\sigma}_m^2, \frac{1}{K} \tilde{\sigma}_m^4\right], \quad (16)$$

$$195 r_{mn} | \mathcal{H}_1 \sim \mathcal{CN}\left[\rho_i \sigma_{sh}^2, \frac{1}{K} \tilde{\sigma}_m^2 \tilde{\sigma}_n^2\right]. \quad (17)$$

196 *Proof:* Due to the space limitation, the proof is integrated  
197 in the supplementary material. ■

198 According to (16), we have

$$199 \mathbb{E}[T_0 | \mathcal{H}_1] = \sum_{m=1}^M \mathbb{E}[T_{mm} | \mathcal{H}_1] = \sum_{m=1}^M \tilde{\sigma}_m^2, \quad (18)$$

$$200 \mathbb{V}[T_0 | \mathcal{H}_1] = \sum_{m=1}^M \mathbb{V}[T_{mm} | \mathcal{H}_1] = \frac{1}{K} \sum_{m=1}^M \tilde{\sigma}_m^4. \quad (19)$$

201 It is obvious that  $\text{Re}(r_{mn})$  and  $\text{Im}(r_{mn})$  is independent of  
202 each other when the SNR is low. Thus, the amplitude  $|r_{mn}|$

follows the Rician distribution  $\mathcal{R}(\nu, \mathcal{V})$  with  $\nu = |\rho_i| \sigma_{sh}^2$  and  
 $\mathcal{V} = \sqrt{\frac{1}{2K} \tilde{\sigma}_m^2 \tilde{\sigma}_n^2}$ . We then have

$$\mathbb{E}(|r_{mn}|) = \mathcal{V} \sqrt{\frac{\pi}{2}} \Psi\left(-\frac{\nu^2}{2\mathcal{V}^2}\right), \quad (20)$$

$$\mathbb{E}(|r_{mn}|^2) = 2\mathcal{V}^2 + \nu^2, \quad (21)$$

which produces  $T_i$  for  $i = 1, \dots, M-1$ ,

$$\mathbb{E}[T_i | \mathcal{H}_1] = \sum_{m=1}^{M-i} \sqrt{\frac{\pi}{4K}} \tilde{\sigma}_m \tilde{\sigma}_{m+i} \Psi\left(-\frac{K \sigma_{sh}^4 |\rho_i|^2}{\tilde{\sigma}_m^2 \tilde{\sigma}_{m+i}^2}\right), \quad (22)$$

$$\begin{aligned} \mathbb{V}[T_i | \mathcal{H}_1] &= \sum_{m=1}^{M-i} \left[ \frac{\tilde{\sigma}_m^2 \tilde{\sigma}_{m+i}^2}{K} + |\rho_i|^2 \sigma_{sh}^4 \right. \\ &\quad \left. - \frac{\pi}{4K} \tilde{\sigma}_m^2 \tilde{\sigma}_{m+i}^2 \Psi^2\left(-\frac{K \sigma_{sh}^4 |\rho_i|^2}{\tilde{\sigma}_m^2 \tilde{\sigma}_{m+i}^2}\right) \right]. \quad (23) \end{aligned}$$

Combining (18), (19), (22) and (23) yields the mean (denoted  
by  $\mu_1$ ) and variance (denoted by  $\sigma_1^2$ ) of  $T_{\text{IWCD}}$  under  $\mathcal{H}_1$ ,  
respectively, as

$$\begin{aligned} \mu_1 &= \sum_{i=0}^{M-1} \mathbb{E}[\omega_i T_i | \mathcal{H}_1] = \omega_0 \sum_{m=1}^M \tilde{\sigma}_m^2 \\ &\quad + \sum_{i=1}^{M-1} \omega_i \sum_{m=1}^{M-i} \sqrt{\frac{\pi}{4K}} \tilde{\sigma}_m \tilde{\sigma}_{m+i} \Psi\left(-\frac{K \sigma_{sh}^4 |\rho_i|^2}{\tilde{\sigma}_m^2 \tilde{\sigma}_{m+i}^2}\right), \quad (24) \end{aligned}$$

$$\begin{aligned} \sigma_1^2 &= \sum_{i=0}^{M-1} \mathbb{V}[\omega_i T_i | \mathcal{H}_1] = \frac{\omega_0^2}{K} \sum_{m=1}^M \tilde{\sigma}_m^4 + \sum_{i=1}^{M-1} \omega_i^2 \sum_{m=1}^{M-i} \left[ \frac{\tilde{\sigma}_m^2 \tilde{\sigma}_{m+i}^2}{K} \right. \\ &\quad \left. + |\rho_i|^2 \sigma_{sh}^4 - \frac{\pi}{4K} \tilde{\sigma}_m^2 \tilde{\sigma}_{m+i}^2 \Psi^2\left(-\frac{K \sigma_{sh}^4 |\rho_i|^2}{\tilde{\sigma}_m^2 \tilde{\sigma}_{m+i}^2}\right) \right]. \quad (25) \end{aligned}$$

In view of the CLT, the distribution of IWCD can then be  
approximated as

$$T_{\text{IWCD}} | \mathcal{H}_1 \sim \mathcal{N}(\mu_1, \sigma_1^2). \quad (26)$$

The detection probability can thus be obtained with the given  
threshold  $\lambda$ , as

$$P_d = Q\left(\frac{\lambda - \mu_1}{\sigma_1}\right). \quad (27)$$

### D. Optimal Weights

Several possible performance indices, such as detec-  
tion probability, receiver operating characteristic (ROC)  
curve, asymptotic relative efficiency and deflection coefficient  
(DC) [20], are available for performance optimization of  
a detector, among which, the DC appeals interesting due  
to its easy calculation and near-optimal manner. However,  
it has been pointed out in [20] that the DC might not  
be a good indicator of performance when the sample size  
is very low. To circumvent this drawback, a heuristic but  
efficient approach namely modified deflection coefficient is  
proposed in [17], which measures the variance-normalized  
distance between the centers of two PDFs under hypothe-  
ses  $\mathcal{H}_0$  and  $\mathcal{H}_1$ . The optimal weight vector is able to  
be found with low computational complexity by optimiz-  
ing the MDC. Let  $\boldsymbol{\omega} = [\omega_0, \omega_1, \dots, \omega_{M-1}]^T$ ,  $\boldsymbol{\mu}_i =$   
 $[\mathbb{E}(T_0), \mathbb{E}(T_1), \dots, \mathbb{E}(T_{M-1})]^T | \mathcal{H}_i$ ,  $i = 0, 1$ ,  $\mathbf{f} = \boldsymbol{\mu}_1 - \boldsymbol{\mu}_0$ ,

241 and  $\mathbf{\Lambda} = \text{diag}\{\mathbb{V}(T_0|\mathcal{H}_1), \mathbb{V}(T_1|\mathcal{H}_1), \dots, \mathbb{V}(T_{M-1}|\mathcal{H}_1)\}$ .  
 242 The optimization problem with respect to the maximization of  
 243 MDC can be stated as [17]

$$244 \max_{\boldsymbol{\omega}} d_m^2(\boldsymbol{\omega}) = \frac{(\mu_1 - \mu_0)^2}{\boldsymbol{\omega}^T \mathbf{\Lambda} \boldsymbol{\omega}} = \frac{(\mathbf{f}^T \boldsymbol{\omega})^2}{\boldsymbol{\omega}^T \mathbf{\Lambda} \boldsymbol{\omega}}, \text{ s. t. } |\boldsymbol{\omega}| = 1. \quad (28)$$

245 Define  $\boldsymbol{\omega}' \triangleq \mathbf{\Lambda}^{-\frac{T}{2}} \mathbf{f}$ . Then, the optimal weights  $\boldsymbol{\omega}^o$  follows  
 246 from [17], as

$$247 \boldsymbol{\omega}^o = \frac{\mathbf{\Lambda}^{-\frac{1}{2}} \boldsymbol{\omega}'}{|\mathbf{\Lambda}^{-\frac{1}{2}} \boldsymbol{\omega}'|}. \quad (29)$$

248 Noticing the diagonal structure of  $\mathbf{\Lambda}$  gives

$$249 \boldsymbol{\omega}_{i-1}^o = \frac{f_i}{\Lambda_{ii}} \left[ \sum_{m=1}^M \frac{f_m^2}{\Lambda_{mm}^2} \right]^{-1/2}, \quad i = 1, 2, \dots, M. \quad (30)$$

250 *Remark 1:* For the sake of illustration, we define  $\varsigma_i \triangleq$   
 251  $\rho_i \sigma_{sh}^2$  for  $i = 1, \dots, M-1$ . It is obvious from (30) that the  
 252 acquisition of optimal weights involve the prior knowledge  
 253  $(\sigma_m, \hat{\sigma}_m, \varsigma_i, m = 1, 2, \dots, M, i = 1, \dots, M-1)$  of the  
 254 observed data under both hypotheses, which is difficult to  
 255 obtain in practice. Assume that there are  $M \times K$  noise-  
 256 only sample  $[\mathbf{x}^{(0)}(1), \dots, \mathbf{x}^{(0)}(K)]$  (the noise-only sample  
 257 are available in possible [21]) and noise-bearing sample  
 258  $[\mathbf{x}^{(1)}(1), \dots, \mathbf{x}^{(1)}(K)]$ , the relevant unknown parameters can  
 259 thus be estimated, i.e.,

$$260 \hat{\sigma}_m^2 = \frac{1}{K} \sum_{k=1}^K \mathbf{x}_m^{(0)}(k) (\mathbf{x}_m^{(0)}(k))^*, \quad (31)$$

$$261 \hat{\sigma}_m^2 = \frac{1}{K} \sum_{k=1}^K \mathbf{x}_m^{(1)}(k) (\mathbf{x}_m^{(1)}(k))^*, \quad (32)$$

$$262 \hat{\varsigma}_i = \frac{1}{K(M-i)} \sum_{k=1}^K \sum_{m=1}^{M-i} \mathbf{x}_m^{(1)}(k) (\mathbf{x}_{m+i}^{(1)}(k))^*. \quad (33)$$

263 In such case, the estimated optimal weights are  
 264 computed as

$$265 \hat{\boldsymbol{\omega}}_{i-1}^o = \frac{\hat{f}_i}{\hat{\Lambda}_{ii}} \left[ \sum_{m=1}^M \frac{\hat{f}_m^2}{\hat{\Lambda}_{mm}^2} \right]^{-1/2}, \quad i = 1, 2, \dots, M. \quad (34)$$

266 where

$$267 \hat{f}_1 = \sum_{m=1}^M (\hat{\sigma}_m^2 - \hat{\sigma}_m^2), \quad \hat{\Lambda}_{11} = \frac{1}{K} \sum_{m=1}^M \hat{\sigma}_m^4, \quad (35)$$

$$268 \hat{f}_i = \sqrt{\frac{\pi}{4K}} \sum_{m=1}^{M-i+1} \left[ \hat{\sigma}_m \hat{\sigma}_{m+i-1} \Psi \left( -\frac{K |\hat{\varsigma}_{i-1}|^2}{\hat{\sigma}_m^2 \hat{\sigma}_{m+i-1}^2} \right) \right. \\ \left. - \hat{\sigma}_m \hat{\sigma}_{m+i-1} \right], \quad i = 2, 3, \dots, M, \quad (36)$$

$$270 \hat{\Lambda}_{ii} = \sum_{m=1}^{M-i+1} \left[ \frac{\hat{\sigma}_m^2 \hat{\sigma}_{m+i-1}^2}{4K} \left( 4 - \pi \Psi^2 \left( -\frac{K |\hat{\varsigma}_{i-1}|^2}{\hat{\sigma}_m^2 \hat{\sigma}_{m+i-1}^2} \right) \right) \right. \\ \left. + |\hat{\varsigma}_{i-1}|^2 \right], \quad i = 2, 3, \dots, M. \quad (37)$$

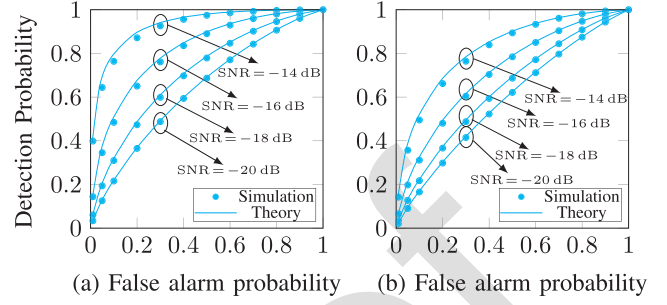


Fig. 1. Verification of theoretical results. (a) uniform noise with  $K = 400$ ,  $M = 6$  and  $\rho = 0.7 + 0.1\iota$ ; (b)  $K = 300$ ,  $M = 4$  and  $\rho = 0.6 + 0.2\iota$  with non-uniform noise variance  $[-1, 0, 1.5, -0.5]$  dB.

AQ4

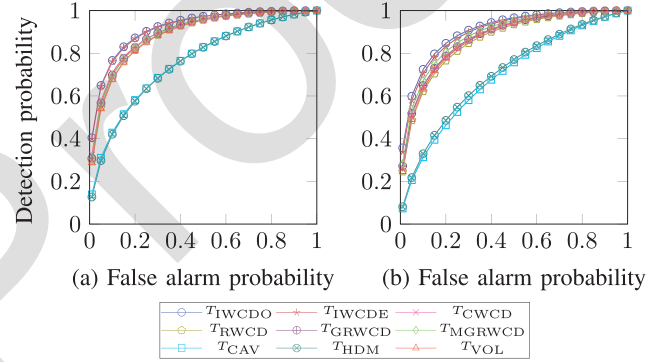


Fig. 2. Comparison of ROC curve with  $K = 500$ ,  $M = 4$  and  $\text{SNR} = -14$  dB. (a) uniform noise with  $\rho = 0.8 + 0.4\iota$ ; (b) non-uniform noise variance  $[0.3, -0.4, -0.7, 0.8]$  dB with  $\rho = 0.7 + 0.3\iota$ .

#### IV. NUMERICAL RESULTS

272

273 This section provides numerical examples to validate the  
 274 theoretical analyses and compare the performance of the  
 275 proposed IWCDs obtained by the optimal weights (30)  
 276 (IWCD) and estimated weights (34) (IWUDE), to the four  
 277 WCDs, namely CWCD [11], RWCD [12], GRWCD ( $p =$   
 278  $\frac{1}{4}$ ) [13], MGRWCD ( $p = \frac{1}{4}$ ) [13], as well as three popular  
 279 competitors, namely CAV [6], VOL [7], HDM [8]. In general,  
 280 the noise power is assumed to be one for uniform noise and  
 281 the average noise power is set to be one for non-uniform noise.

282 Fig. 1 validates the asymptotic expressions of  $P_f$  (14) and  
 283  $P_d$  (27) obtained via the optimal weights (30), by comparing  
 284 the theoretical and simulated ROC curves. The parameter setup  
 285 is  $\rho = 0.7 + 0.1\iota$ ,  $K = 400$  and  $M = 6$  for uniform noise and  
 286  $\rho = 0.6 + 0.2\iota$ ,  $K = 300$  and  $M = 4$  for non-uniform noise  
 287 with variance  $[-1, 0, 1.5, -0.5]$  dB, both with respect to four  
 288 values of SNR  $\in \{-14, -16, -18, -20\}$  dB. As expected, the  
 289 theoretical values agree well with the simulation counterparts,  
 290 thus verifying the correctness of our derived results.

291 Fig. 2 depicts the ROC curve of our proposed IWCD  
 292 methods in comparison with other seven detectors for  $M = 4$ ,  
 293  $K = 500$  and  $\text{SNR} = -14$  dB. Two values of high antenna  
 294 correlation,  $\rho = 0.8 + 0.4\iota$  with uniform noise variance and  
 295  $\rho = 0.7 + 0.3\iota$  with non-uniform noise variance  $[0.3, -0.4,$   
 296  $-0.7, 0.8]$  dB, are considered in Fig. 2 (a) and Fig. 2 (b),  
 297 respectively. It is clear that IWUDE of estimated weights  
 298 performs comparably with IWCD of optimal weights, both  
 299 of which perform better than that of comparison approaches.

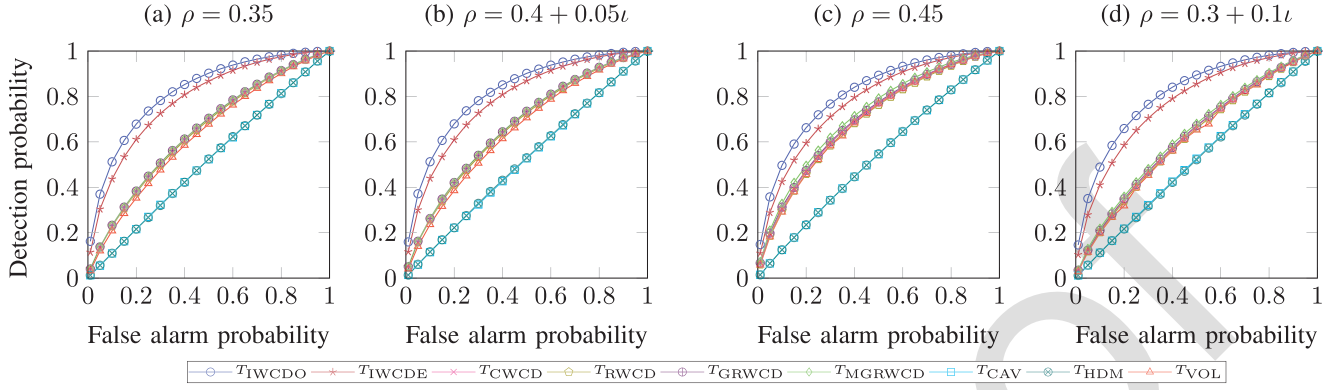


Fig. 3. Comparison of ROC curve for all considered detectors with  $K = 300$ ,  $M = 6$  and  $\text{SNR} = -15$  dB. (a) uniform noise; (b) uniform noise; (c) non-uniform noise with variance  $[1, -0.5, 0.1, -1.2, 0.6, 0]$  dB. (d) non-uniform noise with variance  $[1, -0.5, 0.1, -1.2, 0.6, 0]$  dB.

Fig. 3 draws the detection performance with respect to ROC curve, of all considered detectors in the case where the correlation across the receiver antennas is low. Simulation parameters are set as  $K = 300$ ,  $M = 6$  and  $\text{SNR} = -15$  dB. Four correlation coefficients in the forms of real value and complex value are considered for both the uniform and non-uniform background noise. Specifically, for the case where noise variance is identical, Fig. 3 (a) and Fig. 3 (b) shows the results corresponding to  $\rho = 0.35$  and  $\rho = 0.4 + 0.05\tau$ , respectively; whereas the results for  $\rho = 0.45$  and  $\rho = 0.3 + 0.1\tau$  in the scenarios of non-uniform noise are plotted in Fig. 3 (c) and Fig. 3 (d), respectively. We can deduce from Fig. 3 that our proposed IWCD detectors are superior to other considered methods due to its highest detection probability under a specific false alarm probability. In addition, by comparing Fig. 2 and Fig. 3, the superiority of our proposed detector over other considered detectors can be more evidently observed in the low correlation regime. Compared with optimal weight-aided detector, the estimated weight-aided detector suffers from evident performance loss in the case of low correlation.

## V. CONCLUSION

This letter developed an IWCD detector for cognitive radios with correlated multiple antennas. The proposed method depending on the arbitrary volatile weights, possesses more freedom than the traditional WCDs. The analytic forms with respect to the probabilities of false alarm and detection were derived, facilitating us to determine the optimal weights by maximizing the MDC. Besides, a proper estimator for the optimal weights was devised with the available samples. The superiority of the proposed detector over other state-of-the-art methods was shown via extensive numerical examples.

## REFERENCES

[1] W. Zhao, S. S. Ali, M. Jin, G. Cui, N. Zhao, and S.-J. Yoo, "Extreme eigenvalues-based detectors for spectrum sensing in cognitive radio networks," *IEEE Trans. Commun.*, vol. 70, no. 1, pp. 538–551, Jan. 2022.

[2] M. Ali, M. N. Yasir, D. M. S. Bhatti, and H. Nam, "Optimization of spectrum utilization efficiency in cognitive radio networks," *IEEE Wireless Commun. Lett.*, vol. 12, no. 3, pp. 426–430, Mar. 2023.

[3] H. Ma, X. Yuan, L. Zhou, B. Li, and R. Qin, "Joint block support recovery for sub-Nyquist sampling cooperative spectrum sensing," *IEEE Wireless Commun. Lett.*, vol. 12, no. 1, pp. 85–88, Jan. 2023.

[4] A. Gao, C. Du, S. X. Ng, and W. Liang, "A cooperative spectrum sensing with multi-agent reinforcement learning approach in cognitive radio networks," *IEEE Commun. Lett.*, vol. 25, no. 8, pp. 2604–2608, Aug. 2021.

[5] R. Tandra and A. Sahai, "SNR walls for signal detection," *IEEE Sensors J. Sel. Topics Signal Process.*, vol. 2, no. 1, pp. 4–17, Feb. 2008.

[6] Y. Zeng and Y.-C. Liang, "Spectrum-sensing algorithms for cognitive radio based on statistical covariances," *IEEE Trans. Veh. Technol.*, vol. 58, no. 4, pp. 1804–1815, May 2009.

[7] L. Huang, C. Qian, Y. Xiao, and Q. Zhang, "Performance analysis of volume-based spectrum sensing for cognitive radio," *IEEE Trans. Wireless Commun.*, vol. 14, no. 1, pp. 317–330, Jan. 2015.

[8] L. Huang, Y. Xiao, H. C. So, and J. Fang, "Accurate performance analysis of hadamard ratio test for robust spectrum sensing," *IEEE Trans. Wireless Commun.*, vol. 14, no. 2, pp. 750–758, Feb. 2015.

[9] J. Xie, J. Fang, C. Liu, and X. Li, "Deep learning-based spectrum sensing in cognitive radio: A CNN-LSTM approach," *IEEE Commun. Lett.*, vol. 24, no. 10, pp. 2196–2200, Oct. 2020.

[10] C. Liu, J. Wang, X. Liu, and Y.-C. Liang, "Deep CM-CNN for spectrum sensing in cognitive radio," *IEEE J. Sel. Areas Commun.*, vol. 37, no. 10, pp. 2306–2321, Oct. 2019.

[11] M. Jin, Q. Guo, J. Xi, Y. Li, Y. Yu, and D. Huang, "Spectrum sensing using weighted covariance matrix in Rayleigh fading channels," *IEEE Trans. Veh. Technol.*, vol. 64, no. 11, pp. 5137–5148, Nov. 2015.

[12] A.-Z. Chen and Z.-P. Shi, "A real-valued weighted covariance-based detection method for cognitive radio networks with correlated multiple antennas," *IEEE Commun. Lett.*, vol. 22, no. 11, pp. 2290–2293, Nov. 2018.

[13] A.-Z. Chen, Z.-P. Shi, and J. Xiong, "Generalized real-valued weighted covariance-based detection methods for cognitive radio networks with correlated multiple antennas," *IEEE Access*, vol. 7, pp. 34373–34382, 2019.

[14] A. Winkelbauer, "Moments and absolute moments of the normal distribution," 2012, *arXiv:1209.4340*.

[15] A. Nafkha and B. Aziz, "Closed-form approximation for the performance of finite sample-based energy detection using correlated receiving antennas," *IEEE Wireless Commun. Lett.*, vol. 3, no. 6, pp. 577–580, Dec. 2014.

[16] A. W. V. D. Vaart, *Asymptotic Statistics* (Cambridge Series in Statistical and Probabilistic Mathematics). Cambridge, U.K.: Cambridge Univ. Press, 1998.

[17] Z. Quan, S. Cui, and A. H. Sayed, "Optimal linear cooperation for spectrum sensing in cognitive radio networks," *IEEE J. Sel. Topics Signal Process.*, vol. 2, no. 1, pp. 28–40, Feb. 2008.

[18] A.-Z. Chen, Z.-P. Shi, H. Sun, Z.-Q. He, F. Bu, and D. Yang, "A low-complexity spectrum sensing method for noncircular signal in cognitive radio networks with multiple receive antennas," *IEEE Commun. Lett.*, vol. 23, no. 7, pp. 1190–1193, Jul. 2019.

[19] "Rayleigh distribution." [Online]. Available: [https://en.jinzhao.wiki/wiki/Rayleigh\\_distribution](https://en.jinzhao.wiki/wiki/Rayleigh_distribution)

[20] S. A. Kassam, *Signal Detection in Non-Gaussian Noise*. New York, NY, USA: Springer, 2012.

[21] V. Rakovic, D. Denkovski, V. Atanasovski, P. Mähönen, and L. Gavrilovska, "Capacity-aware cooperative spectrum sensing based on noise power estimation," *IEEE Trans. Commun.*, vol. 63, no. 7, pp. 2428–2441, Jul. 2015.